

Non-volatile, electric control of magnetism in Mn-substituted ZnO

Cite as: Appl. Phys. Lett. **104**, 062409 (2014); <https://doi.org/10.1063/1.4865428>

Submitted: 27 December 2013 . Accepted: 30 January 2014 . Published Online: 11 February 2014

X. L. Wang, Q. Shao, C. W. Leung, R. Lortz, and A. Ruotolo



View Online



Export Citation



CrossMark

ARTICLES YOU MAY BE INTERESTED IN

[Magnetism as a probe of the origin of memristive switching in p-type antiferromagnetic NiO](#)
Applied Physics Letters **103**, 223508 (2013); <https://doi.org/10.1063/1.4834795>

[Coexistence of electric field controlled ferromagnetism and resistive switching for TiO₂ film at room temperature](#)

Applied Physics Letters **107**, 062404 (2015); <https://doi.org/10.1063/1.4928537>

[Resistive switching phenomena: A review of statistical physics approaches](#)

Applied Physics Reviews **2**, 031303 (2015); <https://doi.org/10.1063/1.4929512>

Lock-in Amplifiers
up to 600 MHz



Watch



Non-volatile, electric control of magnetism in Mn-substituted ZnO

X. L. Wang,^{1,2} Q. Shao,¹ C. W. Leung,³ R. Lortz,⁴ and A. Ruotolo^{1,a)}

¹Department of Physics and Materials Science, Device Physics Group, City University of Hong Kong, Kowloon, Hong Kong SAR, China

²State Key Laboratory of Superlattices and Microstructures, Institute of Semiconductors, Chinese Academy of Sciences, Beijing 100083, China

³Department of Applied Physics and Materials Research Centre, The Hong Kong Polytechnic University, Hung Hom, Kowloon, Hong Kong SAR, China

⁴Department of Physics, The Hong Kong University of Science and Technology, Clear Water Bay, Hong Kong SAR, China

(Received 27 December 2013; accepted 30 January 2014; published online 11 February 2014)

We show that the magnetic properties of a dilute semiconductor oxide can be altered in a reversible and non-volatile manner by the application of an electric field. The selected ferromagnetic oxide was manganese-substituted zinc oxide. Bipolar resistive memory switching was induced in the film sandwiched between two metallic electrodes. The bistable switching of the resistive state was accompanied by a bistable switching of the magnetic moment. The scalability of the system was investigated by fabricating devices with lateral size down to 400 nm. © 2014 AIP Publishing LLC. [<http://dx.doi.org/10.1063/1.4865428>]

The electrical control of the magnetic properties of a material is a fascinating possibility. It has indeed been demonstrated that large electric fields, applied through an insulating gate, can alter the magnetic properties of ferromagnetic semiconductor films,¹⁻⁴ as well as ferromagnetic metallic films.⁵⁻⁸ In semiconductors, the effect relies on the capability of the electric field to alter the distribution profile of the electrical carriers, whereas in metallic films the electric field alters the magnetocrystalline anisotropy at the surfaces of the films. In both cases, the application of a large electric field is required. Besides, when the voltage at the gate is removed, the system returns in its original magnetic state. However, it would be desirable to have a material that retains the induced magnetic state when the electric field is removed. In other words, the system should behave as a memristor,⁹⁻¹¹ in which the state variable is the magnetic moment instead of, or in addition to, the resistance.

For this purpose, Mn-substituted ZnO (ZMO) provides a unique opportunity to engineer such a system. This is because, in this compound, magnetism is due to the formation of bound polarons,^{12,13} and therefore, the magnetic moment is a function of the concentration of oxygen vacancies, which provide the majority of the carriers. At the same time, ZMO is known¹⁴ to show interface-type memristive switching, which means oxygen vacancies can be uniformly displaced under the action of an applied electric field.

Here, we demonstrate that a non-volatile electrical switching of resistance and magnetic moment coexist in memristive devices based on ZMO. The oxide films were sandwiched between two metallic electrodes for electrical connection. A bipolar electric field was used to switch the resistance between two stable states. The magnetic characterization of large film-devices showed that different resistive states correspond to different magnetic states.

The studied system consists of 2% Mn-substituted ZnO films sandwiched between two Pt electrodes (Fig. 1(a)). The

trilayers were grown at room temperature, without breaking vacuum, on Al₂O₃ (0001) crystal substrates by using a pulsed KrF excimer laser ($\lambda = 248$ nm) with a repetition rate of 10 Hz and energy 300 mJ. The Pt films were grown in high vacuum (10^{-5} millibar) whereas the oxide films were grown in 0.4 millibar oxygen partial pressure. A complete characterization of the oxide films has been published elsewhere.^{15,16}

We prepared both unpatterned Pt (100 nm)/MnZnO (t nm)/Pt (200 nm) film-devices of size 5 mm^2 and $t = 120, 360, 600$ nm and patterned devices with $t = 120$ nm and size ranging from $0.4 \times 0.4 \mu\text{m}^2$ to $200 \times 200 \mu\text{m}^2$. Devices were patterned out of Pt (100 nm)/MnZnO (120 nm)/Pt (20 nm) trilayers by using standard lithographic processes. Photolithography and electron beam lithography were employed, respectively, for the fabrication of micron and sub-micron devices. The devices were isolated one from the other by sputter-deposited SiO₂. A 200 nm-thick Pt counter-electrode was deposited and defined by lift-off. The devices could be independently biased. In the following, positive current means current flowing from the bottom to the top Pt electrode.

Fig. 1 shows the typical electrical behavior of an unpatterned film-device with $t = 120$ nm. The as-prepared devices showed a rectifying current-voltage (I - V) characteristic (Fig. 1(b)), the polarity of which revealed that the electrical behavior was dominated by a Schottky-like interface between the bottom Pt and the ZMO. Atomic force microscope measurements conducted on single Pt and Pt/ZMO bilayers showed that the roughness at the bottom Pt/ZMO interface was 0.4 nm, whereas the roughness at the top ZMO/Pt interface was one order of magnitude larger. It is well known¹⁷ that the formation of Schottky contacts at metal/ZnO interfaces requires sharp interfaces. As the interface roughness increases, so does the number of ZnO surface defects due to surface termination. These surface defects behave as electrically active sites in the depletion layer, therefore reducing the barrier height. In agreement with this

^{a)}Electronic mail: aruotolo@cityu.edu.hk

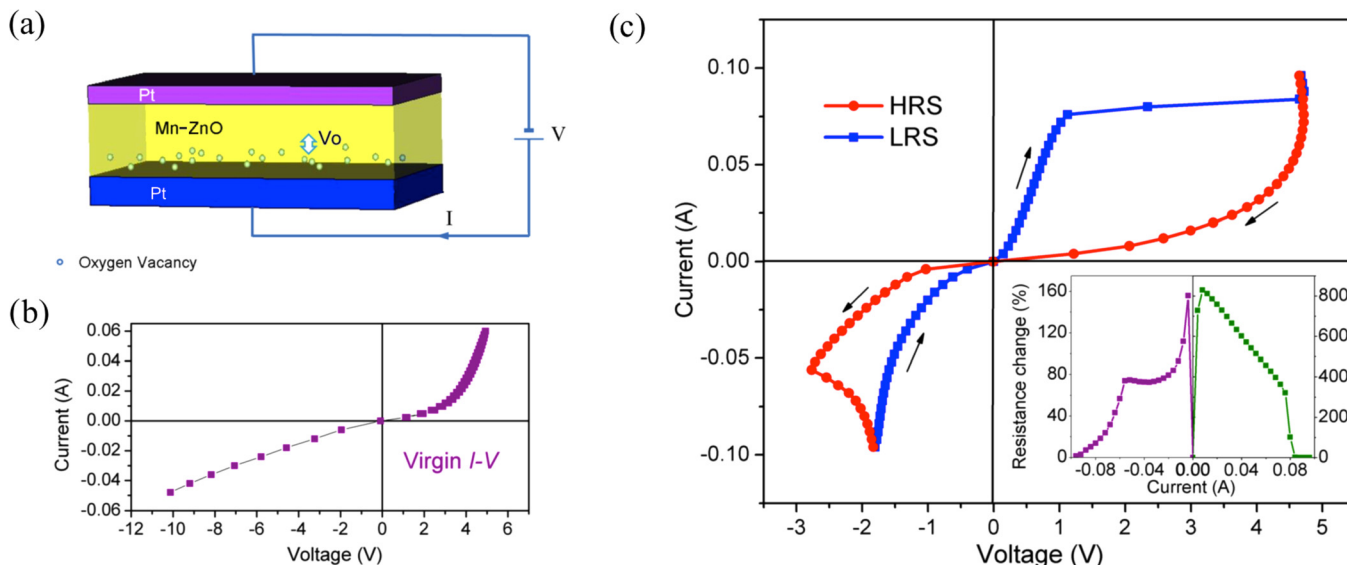


FIG. 1. (a) Schematic representation of the studied system; (b) The as-grown $I-V$ characteristic of a 5 mm^2 -wide, 120 nm -thick $\text{Zn}_{0.98}\text{Mn}_{0.02}\text{O}$ film device; (c) Bipolar d.c. $I-V$ switching operation of the same film device. The inset shows the current dependence of the resistance change ratio, as calculated from the bipolar switching loop.

scenario, in our system a Schottky-like barrier is formed at the bottom interface with the top interface behaving as an ohmic contact.

After an irreversible forming step, which occurs at $\sim 10 \text{ V}$ in reverse bias, the $I-V$ curve becomes hysteretic (Fig. 1(c)), with a change of resistance between the two states as high as 830%. When a reverse threshold current is reached, the $I-V$ shows a negative differential resistance, a typical feature of ionic memristors,^{18–24} and its resistance decreases with increasing current. When a forward threshold current is reached the system switches sharply from a low resistive state (LRS) to a high resistive state (HRS). The hysteresis is stable over repeated sweeps.

Electroresistive switching in oxide semiconductors can have different physical origins. In order to identify the dominant physical mechanism behind the resistive switching in our devices, we first compared the hysteretic $I-V$ curves of film devices with different thicknesses of the semiconducting film (Fig. 2). The threshold voltage increases with the film thickness but not the switching threshold current. This suggests that the effect is confined near the Schottky interface

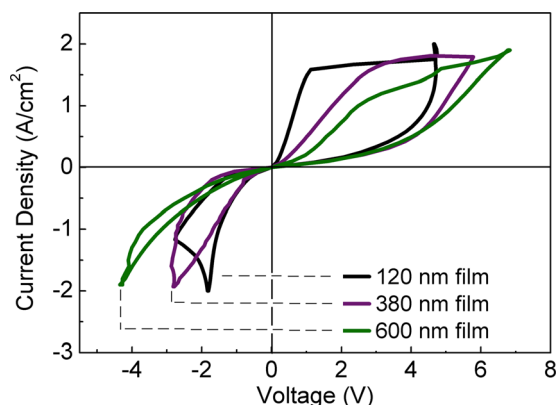


FIG. 2. Resistive switching of devices with different $\text{Zn}_{0.98}\text{Mn}_{0.02}\text{O}$ thicknesses.

and increasing the film thickness only increases the series resistance. In order to understand whether the effect is uniform under the interface, we fixed the film thickness at 120 nm and patterned devices of size ranging from $0.4 \times 0.4 \mu\text{m}^2$ to $200 \times 200 \mu\text{m}^2$. The typical $I-V$ characteristic of the patterned devices was very similar in shape to that measured in extended films (Fig. 3 inset). The log-log plot of the device static resistance as a function of the area (Fig. 3) shows a typical ohmic relationship, with a linear negative slope. This behavior confirms that the effect is uniform under the interface and it is not due to the formation of nano-filaments. In fact, since nano-filaments provide a short path for the current, the resistance of filamentary-type memristors is weakly dependent on the device size.²⁵ Let us point out that the inset of Fig. 3 shows five consecutive sweeps of the $I-V$. Like in the case of unpatterned film devices, patterned devices show no appreciable degradation of the electrical properties over hundreds of consecutive sweeps.

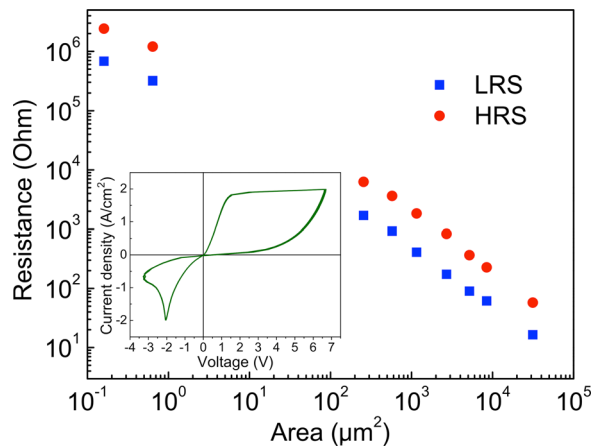


FIG. 3. Area-dependent resistance in the two states. The resistance was measured at a bias current of $J = 1 \text{ A/cm}^2$. Inset shows five consecutive sweeps of the $I-V$ curve of a $75 \times 75 \mu\text{m}^2$ device patterned out from a 120 nm thick $\text{Zn}_{0.98}\text{Mn}_{0.02}\text{O}$.

The capability of the devices to retain the resistive state allows one to disconnect the sample from the electrical circuit and measure the magnetization loop of unpatterned film-devices in a magnetometer. We first measured the full magnetization loop of the samples at room temperature in the two states (Fig. 4). The shown hysteresis loops were extracted from those recorded by subtracting the measured linear contribution of the substrate.

Each substrate contained only one 5 mm^2 device. The loop was first measured at room temperature (Fig. 4(a)) when the sample was in the HRS. Subsequently, the sample was set in the LRS. The electrical circuit was disconnected and the magnetization loop was measured again. We found a reduction of the magnetic moment by 40% in samples with a thickness of ZMO of 120 nm. In order to verify the reversibility of the magnetic switching, the sample was connected again to the electrical circuit to reset it in the HRS. Indeed the original magnetic moment could be totally recovered. A reversible switching of the resistive state corresponds to a reversible switch of the magnetic state. The measurement was repeated at low temperature and in films with different thickness. In Fig. 4(b) we report the magnetization without normalizing to the volume to better show that the change of magnetic moment at saturation (ΔM_S) is independent on the film thickness, thus confirming that the effect is confined to a specific thickness below the Schottky interface, in agreement with the behavior shown in Fig. 2.

Our system bears remarkable resemblance with the voltage-gated devices proposed by other authors¹⁻⁴ to control magnetism in magnetic semiconductors, except non-volatility is added. Similarly to other semiconductors, magnetism in ZMO is carrier mediated.^{12,13} A depletion of the carriers along the film thickness results in a reduction of the magnetic interaction. If the dominant carriers are oxygen vacancies, changing the distribution of the oxygen vacancies results in a change of the magnetic order. In the case of ZMO, coercivity and remanence are always very small and,

therefore, hard to estimate in very thin films. The confinement of the effect over a specific thickness below the interface hinders us from making a comparison between the values of these parameters in the two states, leaving the magnetic moment as the only reliable parameter to describe the magnetic order.

Besides non-volatility, another difference between our system and those previously proposed is that in our case the effect seems to be confined to a specific thickness below the Schottky interface. In similar systems, it has been demonstrated^{21,22} that the effect is confined over the length-scale of the space-charge region (depletion layer) of the Schottky diode, where most of the electric field falls. The width (W) of the depletion layer can be estimated by assuming valid the textbook Schottky diode model. In a Schottky diode²⁶ $W = \sqrt{2\epsilon V_{BO}/qN}$, with V_{BO} the built-in potential and N the carrier concentration. V_{BO} and N can be estimated by measuring the capacitance vs voltage ($C-V$) in reverse bias:^{21,26} $1/C^2 = 2(V_{BO} - V)/qeN$. By assuming a dielectric constant²⁷ $\epsilon = 8.6\epsilon_0$, we estimated $W_{HRS} = 50 \text{ nm}$ and $W_{LRS} = 4 \text{ nm}$, corresponding to built-in potentials $V_{BO,LRS} = 0.5 \text{ V}$ and $V_{BO,HRS} = 0.7 \text{ V}$, and carrier concentrations $N_{HRS} = 2 \times 10^{17} \text{ cm}^{-3}$ and $N_{LRS} = 3 \times 10^{19} \text{ cm}^{-3}$ in the low and high resistive states, respectively. In the film-device with oxide thickness $t = 120 \text{ nm}$, the relative change in width of the depletion layer is $\Delta W/t = (W_{HRS} - W_{LRS})/t \sim W_{HRS}/t = 40\%$, in agreement with the change of magnetic moment. This makes us conclude that when switching to the LRS, only the oxygen vacancies in the layer of width W_{HRS} are displaced and accumulate under the Schottky interface (which becomes quasi-ohmic), leaving a layer of width $W_{HRS} - W_{LRS}$ highly resistive and paramagnetic. Since magnetism in this compound is due to formation of bound magnetic polarons,¹³ i.e., ferromagnetic alignment between Mn^{2+} ions is mediated by oxygen vacancies, depleting this layer of vacancies is equivalent to destroy ferromagnetic order.

Let us finally point out that the presence of the unaffected layer is unavoidable since a neutral region must

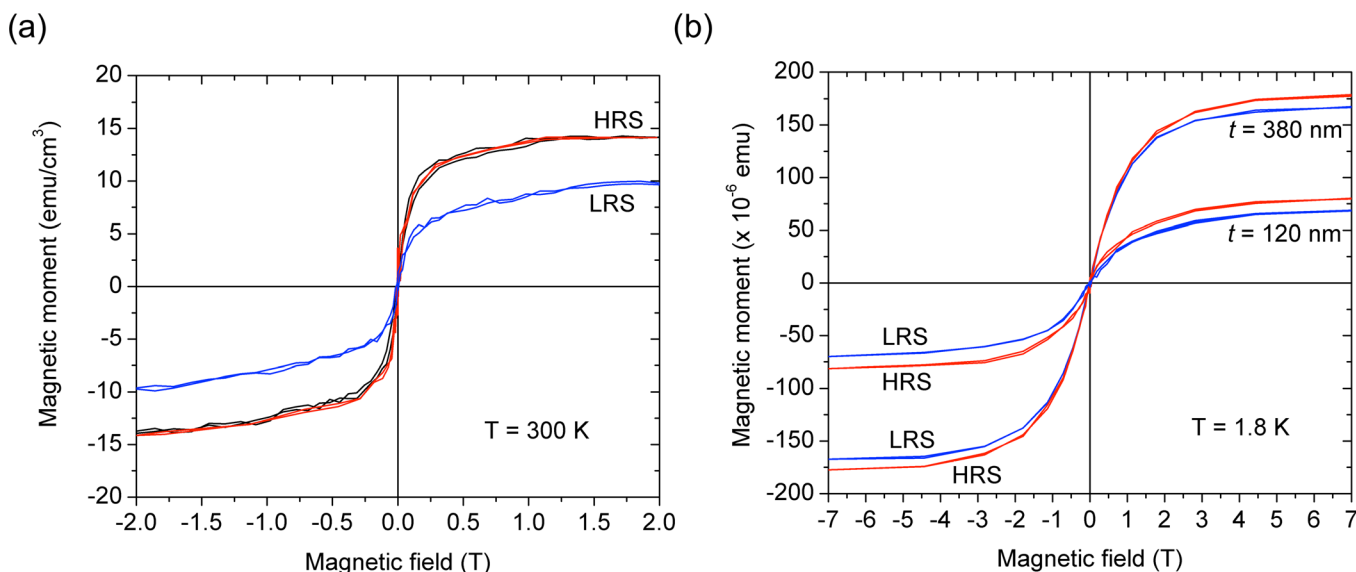


FIG. 4. (a) Magnetization versus in-plane applied field of a 120-nm-thick, 5 mm^2 -wide film device at $T = 300 \text{ K}$ in both resistive states. (b) The same film device measured at $T = 1.8 \text{ K}$ and compared with a 380-nm-thick film device. The magnetization was not normalized to the volume to show the confinement of the effect over the same width, regardless the film thickness.

necessarily exist in a Schottky diode between the space-charge region and the ohmic contact.²⁶ This unaffected region will always contribute with a magnetic background, as well as a series resistance.

In conclusion, we have induced bipolar resistive memory switching in Schottky contacts to Mn-doped ZnO films. Switching the system in the low resistance state is equivalent to deplete the space-charge region of the diode of oxygen vacancies, which are the dominant carriers. Since ferromagnetism in this compound is carrier-mediated, a non-volatile switching of the resistive state coexists with a non-volatile switching of the magnetic moment in the depletion layer of the diode.

The work described in this paper was supported by the Research Grants Council of the Hong Kong Special Administrative Region, China [Grant Nos. CityU102711, CityU 104512, and SEG HKUST03] and by the National Science Foundation of China (NSFC), [Grant No. 11274261]. Financial support from PolyU [5013/08P] is also acknowledged.

- ¹H. Ohno, D. C. F. Matsukura, T. Omiya, E. Abe, T. Dietl, Y. Ohno, and K. Ohtani, *Nature* **408**, 944 (2000).
- ²T. Lottermoser, T. Lonkai, U. Amann, D. Hohlwein, J. Ihlinger, and M. Fiebig, *Nature* **430**, 541 (2004).
- ³D. Chiba, F. Matsukura, and H. Ohno, *Appl. Phys. Lett.* **89**, 162505 (2006).
- ⁴Y. Yamada, K. Ueno, T. Fukumura, H. T. Yuan, H. Shimotani, Y. Iwasa, L. Gu, S. Tsukimoto, Y. Ikuhara, and M. Kawasaki, *Science* **332**, 1065 (2011).
- ⁵M. Weisheit, S. Fahler, A. Marty, Y. Souche, C. Poinignon, and D. Givord, *Science* **315**, 349 (2007).
- ⁶T. Maruyama, Y. Shiota, T. Nozaki, K. Ohta, N. Toda, M. Mizuguchi, A. A. Tulapurkar, T. Shinjo, M. Shiraishi, S. Mizukami, Y. Ando, and Y. Suzuki, *Nat. Nanotechnol.* **4**, 158 (2009).

- ⁷M. Endo, S. Kanai, S. Ikeda, F. Matsukura, and H. Ohno, *Appl. Phys. Lett.* **96**, 212503 (2010).
- ⁸D. Chiba, S. Fukami, K. Shimamura, N. Ishiwata, K. Kobayashi, and T. Ono, *Nat. Mater.* **10**, 853 (2011).
- ⁹L. O. Chua, *IEEE Trans. Circuit Theory* **18**, 507 (1971).
- ¹⁰L. Chua, *Appl. Phys. A* **102**, 765 (2011).
- ¹¹D. B. Strukov, G. S. Snider, D. R. Stewart, and R. S. Williams, *Nature* **453**, 80 (2008).
- ¹²T. Dietl, H. Ohno, F. Matsukura, J. Cibert, and D. Ferrand, *Science* **287**, 1019 (2000).
- ¹³J. M. D. Coey, M. Venkatesan, and C. B. Fitzgerald, *Nat. Mater.* **4**, 173 (2005).
- ¹⁴H. Y. Peng, G. P. Li, J. Y. Ye, Z. P. Wei, Z. Zhang, D. D. Wang, G. Z. Xing, and T. Wu, *Appl. Phys. Lett.* **96**, 192113 (2010).
- ¹⁵X. L. Wang, K. H. Lai, and A. Ruotolo, *J. Alloys Compd.* **542**, 147 (2012).
- ¹⁶X. L. Wang, C. Y. Luan, Q. Shao, A. Pruna, C. W. Leung, R. Lortz, J. A. Zapien, and A. Ruotolo, *Appl. Phys. Lett.* **102**, 102112 (2013).
- ¹⁷L. J. Brillson and Y. Lu, *J. Appl. Phys.* **109**, 121301 (2011).
- ¹⁸G. Dearnaley, A. M. Stoneham, and D. V. Morgan, *Rep. Prog. Phys.* **33**, 1129 (1970).
- ¹⁹T. Fujii, M. Kawasaki, A. Sawa, H. Akoh, Y. Kawazoe, and Y. Tokura, *Appl. Phys. Lett.* **86**, 012107 (2005).
- ²⁰A. Sawa, T. Fujii, M. Kawasaki, and Y. Tokura, *Appl. Phys. Lett.* **85**, 4073 (2004).
- ²¹A. Ruotolo, C. Y. Lam, W. F. Cheng, K. H. Wong, and C. W. Leung, *Phys. Rev. B* **76**, 075122 (2007).
- ²²A. Ruotolo, C. W. Leung, C. Y. Lam, W. F. Cheng, K. H. Wong, and G. P. Pepe, *Phys. Rev. B* **77**, 233103 (2008).
- ²³M.-J. Lee, C. B. Lee, D. Lee, S. R. Lee, M. Chang, J. H. Hur, Y.-B. Kim, C.-J. Kim, D. H. Seo, S. Seo, U.-I. Chung, I.-K. Yoo, and K. Kim, *Nat. Mater.* **10**, 625 (2011).
- ²⁴J. J. Yang, M. D. Pickett, X. Li, D. A. A. Ohlberg, D. R. Stewart, and R. S. Williams, *Nat. Nanotechnol.* **3**, 429 (2008).
- ²⁵R. Waser, R. Dittmann, G. Staikov, and K. Szot, *Adv. Mater.* **21**, 2632 (2009).
- ²⁶C. Y. Chang and S. Sze, *Solid-State Electron.* **13**, 727 (1970).
- ²⁷S. J. Pearton, D. P. Norton, K. Ip, Y. W. Heo, and T. Steiner, *J. Vac. Sci. Technol., B* **22**, 932 (2004).